CONFIGURATION OPTIMIZATION OF A SPLITTING CO_2 TRANSCRITICAL POWER CYCLE IN ENGINE WASTE HEAT RECOVERY: AN EXPERIMENTAL COMPARATIVE STUDY

Ligeng Li[1], Hua Tian[1]*, Lingfeng Shi[2], Yonghao Zhang[2], Xuan Wang[1], Gequn Shu[1]

[1]State Key Laboratory of Engines, Tianjin University, Tianjin, China

[2]Department of Thermal Science and Energy Engineering, University of Science and Technology of China, Hefei, China

*Corresponding Author: thtju@tju.edu.cn

ABSTRACT

Great energy conservation potential has been found in engine waste heat recovery, and CO_2 transcritical power cycle (CTPC) driven by internal combustion engines has been recognized a promising technological path. Traditional recuperative configuration leads to an increase in thermal efficiency but also has an impact on engine exhaust utilization. Hence, based on the CTPC layout with a recuperator, a splitting design is proposed with an additional heater to reduce the irreversibility from the engine exhaust. Experimental investigation was conducted to reveal the splitting performances compared with the basic recuperative layout. Results showed that the predicted net generated power could be increased by 54.8% from 5.4 kW to 8.4 kW in maximum. The engine exhaust utilization could be improved with a lower exhaust outlet temperature. It should also be noted that the thermal efficiency was also improved by 47.5% compared with the baseline although a higher heat absorption was found in the splitting layout.

1 INTRODUCTION

Supercritical or transcritical CO_2 power cycle (s-CO_2 or CTPC) are advanced power cycles in transforming thermal energy into mechanical work and has been widely studied in nuclear (Wu et al., 2020), fossil fuel (Park et al., 2018), concentrating solar power (Cheang et al., 2015), gas turbine (Kim et al., 2016), industrial waste heat (Mondal et al., 2017) and geothermal (Ahmandi et al., 2016). It could be found that several advantages of working fluid CO_2 including high thermal stability, environmentally friendly and nontoxic makes it more and more competitive in future power capacity device (Liu et al., 2019) compared with the Organic rankine cycle system. Also, the materials compatibility and system compactness make it attractive in comparison with water-steam Rankine cycle power plants (Xu et al., 2019).

In the field of engine waste heat recovery, which is supposed to be a promising technology to improve the engine efficiency and has great potential in CO_2 emission reduction, some literatures conducted meaningful configuration optimization when the CO_2 power cycle is utilized as the bottoming cycle to recover the waste heat including engine exhaust and coolant. Chen et al. (2005) compared a recuperative cycle layout driven by an internal combustion engine and studied the thermal efficiency affected by the recuperative effectiveness. More than 50% increase could be found when the recuperator effectiveness reached 60%. Likewise, an increase of 2.4% in thermal efficiency and 2.5% in exergy efficiency has been found in the theoretic analysis with a recuperator by Cayer E et al. (2009). Shu et al. (2016) analysed a synchronize utilization of both exhaust and coolant with a preheater and recuperator. The exhaust utilization may be reduced by less than 30% in part of the operating conditions especially under high expansion inlet temperature. Kim et al. (2017) proposed a splitting CTPC layout to recover the exhaust from a gas turbine when another heater is introduced, and the net power could be increased effectively when recuperative, splitting and cascade configuration layouts were compared.

On one hand, it can be seen that the recuperative layout could increase the internal heat transfer and enhance the thermal efficiency, whereas the engine exhaust utilization rate may be unfortunately decreased since the exhaust could hardly be cooled thoroughly by the heat carrier media with a relatively high recuperative temperature. On the other hand, a splitting branch may produce an effective impact on the system efficiency dealing with the heat source utilization. In addition, limited study is focused on the experimental investigation and the configuration optimization needs to be further verified.
Therefore, in this study, a splitting CTPC experimental system is constructed and thermodynamic performances comparison between the basic recuperative layout and splitting layout is given to reveal and verify the feasibility and superiority when the splitting design is introduced.

2 EXPERIMENTAL FACILITY

2.1 Target Engine

The target engine utilized in this study is an inline four-stroke four-cylinder diesel engine manufactured by Lovol, equipped with the standard measuring and controlling system to ensure the stable operation and data acquisition with great precision. Its main technical parameters are listed in Table 1.

Table 1: Specification of the objective diesel engine

Item	Value
Engine model	4D160-e3P
Displacement	3.99 L
Intake Type	Charge inter-cooling
Bore × Stroke	100 mm × 127 mm
Rated power	118 kW
Rated speed	2500 RPM
Maximum torque	580 N·m

2.2 CTPC system

Fig. 1 and Fig. 2 give the picture and schematic diagram of the 10 kW-scale prototype experimental system, respectively. Main components of the basic recuperative configuration for the engine-driven CTPC are composed of pump, preheater, recuperator, high-temperature gas heater (HTGH), turbine, condenser and reservoir. Since the turbine is still in maintenance, a throttle valve is utilized temporarily to conduct the performances evaluation. The working fluid is firstly pressurized by the pump to achieve the supercritical pressure, and heated consecutively by the preheater, recuperator and HTGH, respectively, to achieve the supercritical temperature recovering the engine coolant, the CO_2 exhaust and engine exhaust. The biggest difference between the splitting and basic recuperative configuration lies in an additional splitting branch with another low-temperature gas heater (LTGH). An obvious advantage of the splitting configuration is making it possible to recover the engine exhaust as much as possible. Meanwhile, the mass flow rate for both branches can be adjusted according to the operation conditions. Main components are summarized in Table 2.

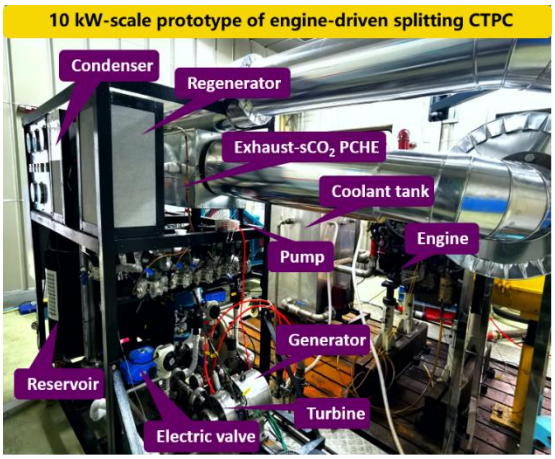

Figure 1: The picture of the experiment facility

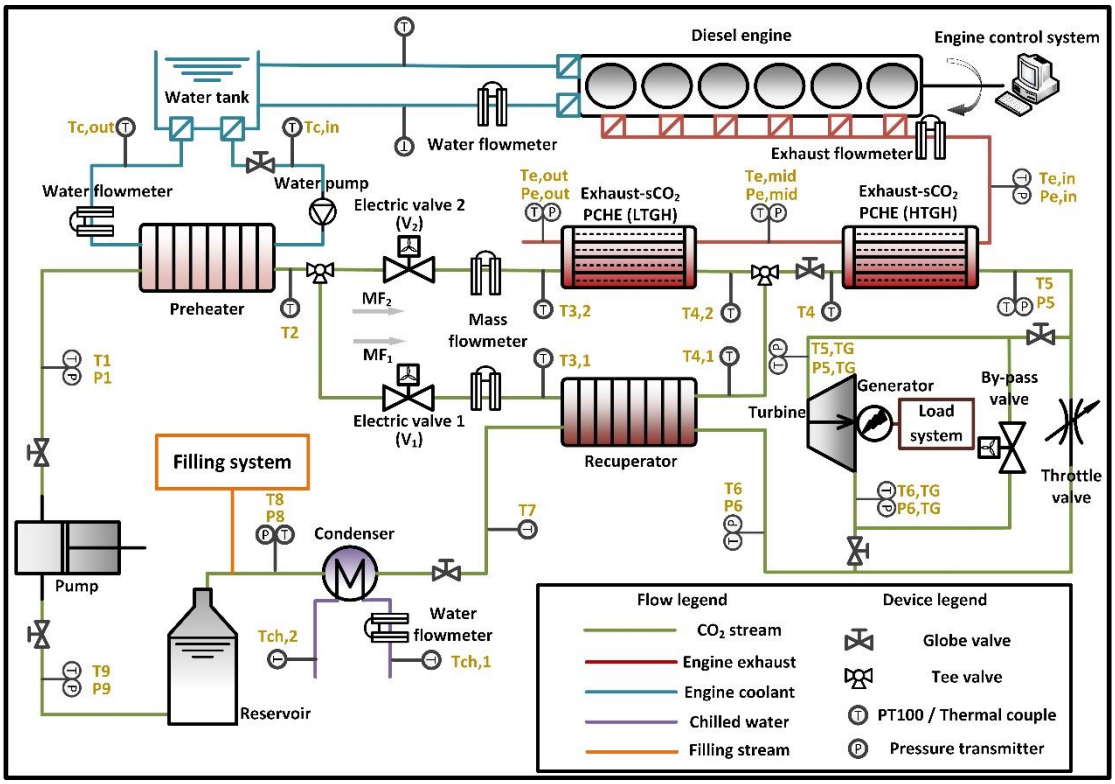

Figure 2: The schematic diagram of the experimental system

Table 2: Technical Specification of main components

Component	Item	Specification
Pump	Type	Reciprocating plunger pump
	Rated flow rate	4 m^3/h
	Maximum pressure	15 MPa
Expander	Type	Partial admission axial turbine
	Design power	15 kW
	Design speed	40,000 RPM

Generator	Type	Synchronous motor
	Connection type	Coaxial
Preheater	Type	Plate
	Area	6.81 m^2
	Flow type	Counter-current
Recuperator	Type	Plate
	Area	9.08 m^2
	Flow type	Counter-current
Exhaust-sCO_2 LTGH	Type	PCHE
	Area	3.00 m^2
	Flow passages	Straight channel
Exhaust-sCO_2 HTGH	Type	PCHE
	Area	5.97 m^2
	Flow passages	Straight channel
Condenser	Type	Plate
	Area	5.90 m^2
	Flow type	Counter-current
Reservoir	Type	Vertical pressure vessel
	Volume	40 L

2.3 Measurement and data acquisition

Fig. 2 has shown all the measurement instrument and relative measuring points, mainly including 21 temperature sensors, 10 pressure transmitters, necessary flowmeters as well as an engine control system. The system design software LABVIEW is also developed with necessary PLC modules coupled to achieve the data acquisition and test rig control. The measurement devices are summarized in Table 3.

Table 3: Type, operating range and accuracy of measurement devices

Measured parameter	Physical principle	Range	Accuracy
Temperature			
Exhaust	Thermocouple Type K	-60-650 °C	±1%
CO_2	Thermal resistance PT100	-200-600 °C	±0.15%
Water	Thermal resistance PT100	-200-600 °C	±0.15%
Pressure			
Exhaust	Differential pressure	0-0.5 MPa	±0.065%
CO_2	Differential pressure	0-16 MPa	±0.065%
Flow rate			
CO_2	Coriolis	0-0.8 kg/s	±0.2%
Coolant	Turbine	1-10 m^3/h	±0.5%
Chilled water	Turbine	1.5-15 m^3/h	±1%

The enthalpy, entropy and specific heat capacity for each state point is calculated through the measured state parameters including the mass flow rate, temperature and pressure, when the reservoir inlet temperature is maintained for at least 2-3 minutes. Properties such as enthalpy, entropy, specific heat capacity and thermodynamic analysis are calculated in Python 3.8 importing the CoolProp (Version 6.4.1). The isentropic efficiencies of the pump and turbine are set to be 0.8 and 0.6, respectively. The equations utilized for heat transfer in exchangers are given below:

For the preheater:

$$\boldsymbol{Q_{pre}=(MF_1+MF_2)\cdot(h_2-h_1)} \quad (1)$$

For the recuperator:

$$\boldsymbol{Q_{rec}=MF_1\cdot(h_{4,1}-h_{3,1})} \quad (2)$$

For the LTGH:

$$Q_{\mathrm{LTGH}}=MF_2\cdot(h_{4,2}-h_{3,2}) \tag{3}$$

For the HTGH:

$$Q_{\mathrm{HTGH}}=(MF_1+MF_2)\cdot(h_5-h_4) \tag{4}$$

The calculated net power and thermal efficiency are calculated below:

$$W_{\mathrm{net,\ prediction}}=(W_t-W_p) \tag{5}$$

$$\eta_{\mathrm{th,\ prediction}}=\frac{W_{\mathrm{net,\ prediction}}}{Q_{\mathrm{in,total}}} \tag{6}$$

where the $Q_{in,\ total}$ represents the total heat absorption rate which is defined below:

$$Q_{\mathrm{in,\ total}}=Q_{\mathrm{pre}}+Q_{\mathrm{LTGH}}+Q_{\mathrm{HTGH}} \tag{7}$$

3 RESULTS AND DISCUSSION

3.1 Experimental process

Fig. 3 represents the experimental process when the opening of the V_1 is changed from 0 to 100%. Corresponding change of the mass flow rate of in each branch is found decided by the valve opening mainly. The recuperative system can be achieved when the valve opening is zero, and an opposite trend in each mass flow rate is found with the increase of the valve opening to achieve splitting design.

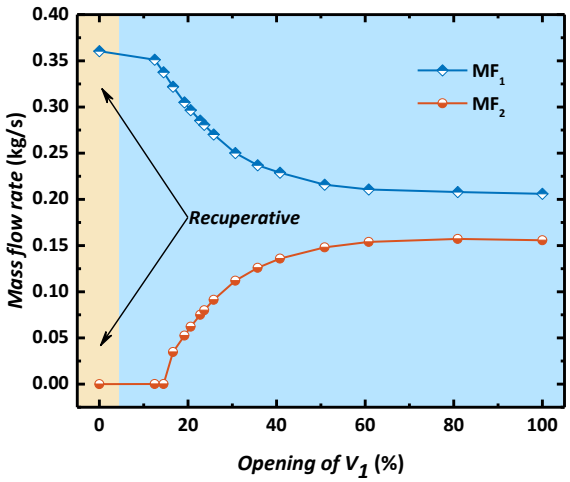

Figure 3: Tendency of the mass flow rate in each branch

Fig. 4 gives the operation parameters of throttle valve inlet pressure and temperature when the same boundary conditions of the heat source and heat sink are kept. Both the T_5 and P_5 increase at first sharply and the decrease gently with the increase of the valve opening. Apparent improvements of operation parameters are found compared with the recuperative system.

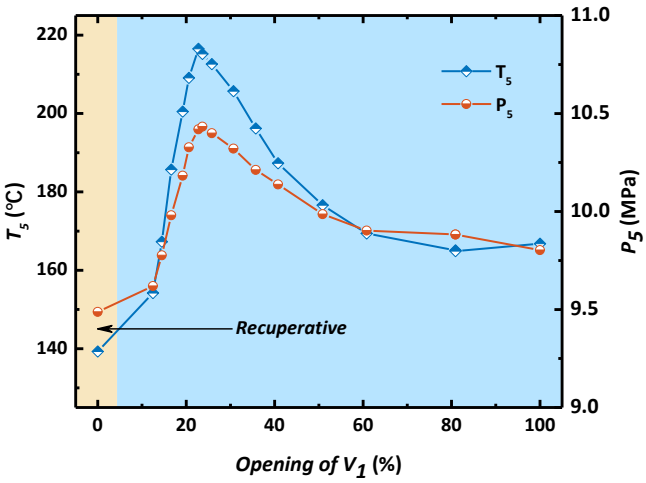

Figure 4: Tendency of the throttle valve inlet operation parameters

3.2 Comparison results

Fig. 5 shows the heat transfer in heater and recuperator for both configurations. Benefited from the additional LTGH, the engine exhaust could be recovered more thoroughly in the splitting configuration with 37.35 kW compared with 31.84 kW in the basic recuperative layout. More apparent distinction is found in heat transfer in recuperator where an increase of 70.67% could be obtained.

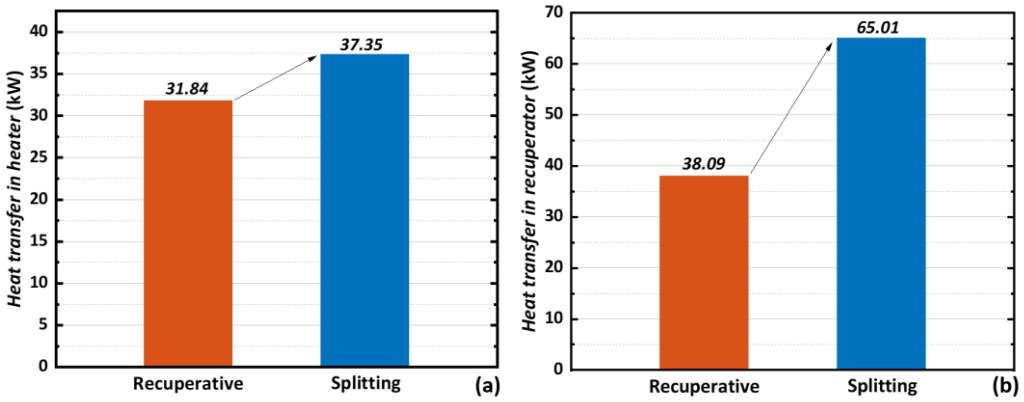

Figure 5: Heat transfer comparison

Fig. 6 shows the operation parameters of T_5 and P_5 when the same pump speed is adopted. Since the heat absorption in recuperative layout is limited by both the heater and recuperator, the throttle valve inlet temperature is much lower than that of the splitting layout, which also leads to the decrease of the power capacity.

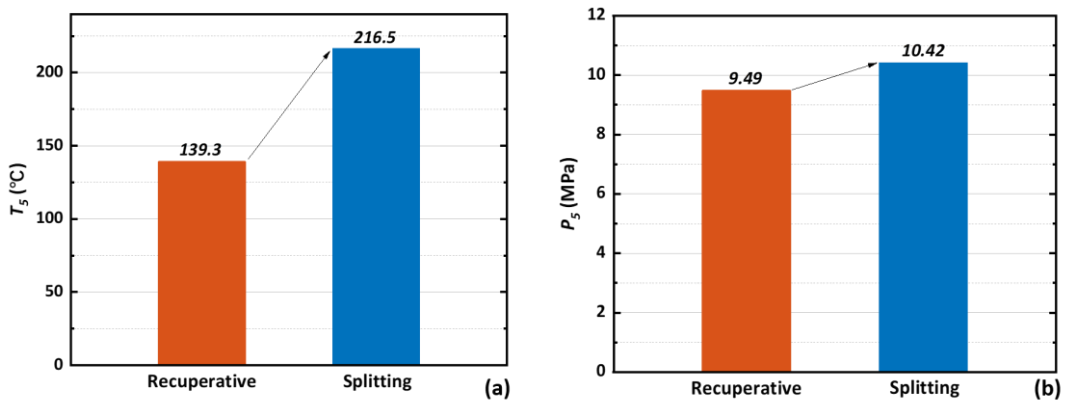

Figure 6: Operation parameters comparison

The comparison of the thermodynamic performances including the net power and thermal efficiency are shown in Fig. 7. Even though the mass flow rate for both configurations is kept the same, the net power and thermal efficiency in the splitting layout is increased by 60.71% and 51.67%, respectively. The main reason can be attributed to a higher average endothermic temperature in the splitting configuration.

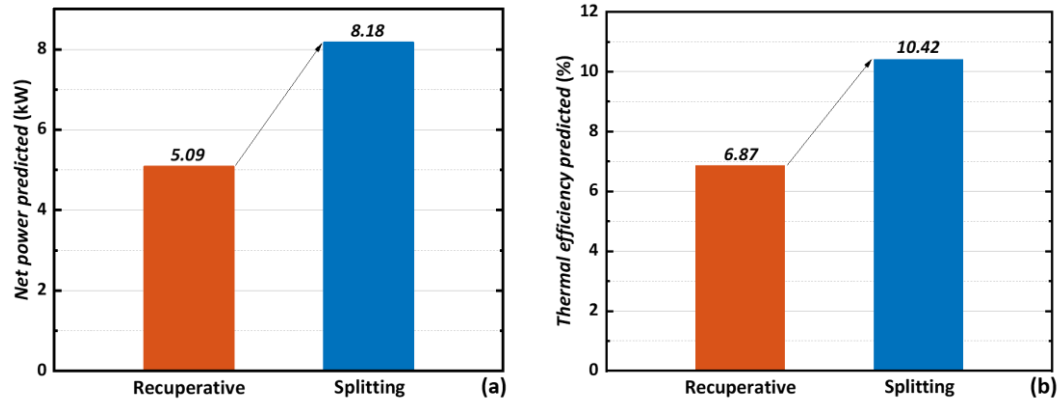

Figure 7: Thermodynamic performances comparison

The total mass flow rate as well as the separate one in each branch is shown in Fig. 8. On one hand, the total mass flow for both configurations is equal to each other since the pump rotational speed is controlled the same value, which is supposed to affect the mass flow rate mainly. By means of the opening of the electric valve in each splitting branch, the working fluid after the preheater is separated into two mass flow rates, one of which still streams through the recuperator, whereas the rest working fluid plays a vital role in recovering the engine exhaust, so that superior thermodynamic performances could be achieved. The optimal splitting mass flow in each branch is 0.28 and 0.08 kg/s, verifying the feasibility and effectiveness when a splitting branch is introduced.

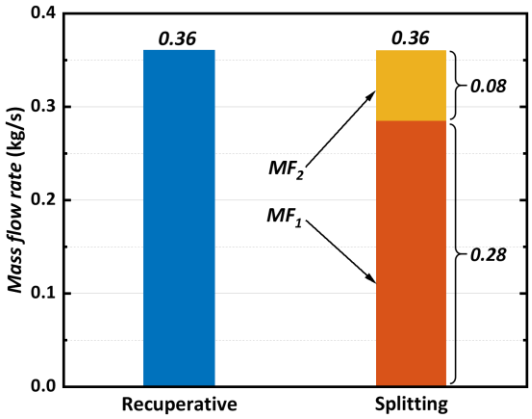

Figure 8: The mass flow rate comparison

The experimental results of operation parameters for both layouts are summarized in Table 4. The results are compared under the same pump speed when the maximum net power predicted for both systems are obtained.

Table 4: Summarization of the operation parameters

Item	Recuperative	Splitting
Temperature (°C)		
T_1	28.7	29.3
T_2	49.1	53.3
$T_{3,1}$	46.5	51.0
$T_{3,2}$	63.0	50.6
$T_{4,1}$	80.4	171.9
$T_{4,2}$	89.3	165.3
T_4	78.3	168.6
T_5	139.3	216.5
T_6	121.6	199.2
T_7	43.2	49.0
T_8	23.6	23.1
T_9	23.0	22.4
Pressure (MPa)		
P_5	9.49	10.42
P_6	6.11	6.04
Mass flow rate (kg/s)		
MF_1	0.360	0.285
MF_2	0	0.075

4 CONCLUSION

In this study, an experiment-based configuration optimization is conducted to make thermodynamic performances comparison between the basic recuperative cycle and proposed splitting cycle and reveal the feasibility and effectiveness of the proposed layout. Two concrete conclusions can be summarized below:

- The splitting design could not only improve the utilization of the engine exhaust, but also increase the heat transfer in the recuperator that contributes to a higher thermal efficiency.

- The mass flow rate streaming through each branch should be adjusted and optimized to achieve a synergistic match of internal CO_2 exhaust and external engine exhaust leading to an increase of 60.71% in net power output.

The future work will be focused on the further performance evaluation when the multiple engine conditions are taken into account to give the further explanation about the splitting control mechanism. Although a throttle valve makes it convenient and easy to control to validate the advantaged of the splitting design, based on the splitting regulation exploration, the turbine will be finally introduced to replace the throttle valve to further reveal the performances of the practical application.

NOMENCLATURE

Abbreviations

MF	mass flow rate	(kg/s)

Symbols

ch	chilled water	(–)
P	pressure	(MPa)
T	temperature	(℃)
V	valve	(–)

Subscript

1-9	state point
c	coolant
e	exhaust
in	inlet
mid	middle
out	outlet

REFERENCES

Wu, P. , Ma, Y., Gao, C., Liu, W., Shan, J., Huang, Y., et al., 2020, A review of research and development of supercritical carbon dioxide Brayton cycle technology in nuclear engineering applications, *Nuclear Engineering and Design*, vol.368: p.110767.

Park, S., Kim, J., Yoon, M., Rhim, D., Yeom, C., 2018, Thermodynamic and economic investigation of coal-fired power plant combined with various supercritical CO2 Brayton power cycle, *Applied Thermal Engineering*, Vol.130: p.611-623.

Cheang, V.T., Hedderwick, R.A., McGregor, C., 2015, Benchmarking supercritical carbon dioxide cycles against steam Rankine cycles for Concentrated Solar Power, *Solar Energy*, vol.113: p.199-211.

Kim, M.S., Ahn, Y., Kim, B., Lee, J.I., 2016, Study on the supercritical CO2 power cycles for landfill gas firing gas turbine bottoming cycle, *Energy*, vol.111: p.893-909.

Mondal, S., De, S., 2017, Power by waste heat recovery from low temperature industrial flue gas by Organic Flash Cycle (OFC) and transcritical-CO2 power cycle: A comparative study through combined thermodynamic and economic analysis, *Energy*, vol.121: p.832-40.

Ahmadi, M.H., Mehrpooya, M., Pourfayaz, F., 2016, Thermodynamic and exergy analysis and optimization of a transcritical CO2 power cycle driven by geothermal energy with liquefied natural gas as its heat sink, *Applied Thermal Engineering*, vol.109: p.640-52.

Liu, Y., Wang, Y., Huang, D., 2019, Supercritical CO2 Brayton cycle: A state-of-the-art review, *Energy*, vol.189: p.115900.

Xu J., Liu C., Sun E., Xie J., Li M., Yang Y., et al.,2019, Perspective of S−CO2 power cycles, *Energy*, vol.186: p.115831.

Chen, Y., Lundqvist, P., Platell, P., 2005, Theoretical research of carbon dioxide power cycle application in automobile industry to reduce vehicle's fuel consumption, *Applied Thermal Engineering*, vol.25, no.14-15: p.2041-2053.

Cayer, E., Galanis, N., Desilets, M., Nesreddine, H., Roy, P., 2009, Analysis of a carbon dioxide transcritical power cycle using a low temperature source, *Applied Energy*, vol.86, no.7-8: p.1055-1063.

Shu, G., Shi, L., Tian, H., Li, X., Huang, G., Chang, L., 2016, An improved CO2-based transcritical Rankine cycle (CTRC) used for engine waste heat recovery, *Applied Energy*, vol.176: p.171-182.

Kim, Y.M., Sohn, J.L., Yoon, E.S., 2017, Supercritical CO 2 Rankine cycles for waste heat recovery from gas turbine, *Energy*, vol.118: p.893-905.

ACKNOWLEDGEMENT

This study is supported by the National Science Fund for Excellent Young Scholars (52022066) and National Natural Science Foundation of China (51906237).